Laplace Beltrami Based Formulation of Corpus Callosum to Ventricle Ratio for the Analysis of Alzheimer's Condition in T1-Weighted MR Images

S. R. Manuskandan[1] and *K. R. Anandh*[2]

1. Karuvee Innovations Pvt. Ltd., Indian Institute of Technology Madras Research Park, Chennai, India
2. The University of Alabama at Birmingham, Birmingham, Alabama
online.manusr@gmail.com, anandhmurali@gmail.com

Abstract— Alzheimer's Disease (AD) is a fatal neurological condition predominated by atrophic changes in brain sub-anatomic regions. Enlargement of lateral ventricle leads to deformations of corpus callosum in Mild Cognitive Impairment (MCI) and AD subjects. However, this phenomenon of shape change has not been comprehensively quantified. In this work, an attempt has been made to analyze the atrophy of corpus callosum (CC) due to the enlargement of lateral ventricles using Laplace Beltrami (LB) eigenvalue features. The images for this study are obtained from a public domain Open Access Series of Imaging Studies (OASIS) database. The lateral ventricles and CC are segmented using a reaction diffusion level set method. LB eigenvalue features are extracted from the segmented images and are statistically analyzed. The CC to Ventricle Ratio (CVR) has been formulated to quantify and differentiate the shape changes in normal, MCI and AD subjects. Results show that LB eigenvalues can capture the shape changes of ventricles and CC in normal, MCI and AD subjects. The newly formulated CVR using LB eigenvalues can quantify the shape changes of CC due to ventricle enlargement and statistically differentiates the normal, MCI and AD subjects ($p < 0.001$). Thus, this study seems to be clinically substantial.

I. Introduction

Alzheimer's Disease (AD) is a slowly developing neurodegenerative disorder that is characterized by cognitive impairment, degenerative pathology, and brain atrophy [1]. It is a common reason for dementia in the elderly and is a global threat to mankind [2]. Severe and rapid decrease in memory is observed in the subjects affected with AD [3]. Although normal aging causes memory loss and dementia, there exists uncertainty in the cognitive decline caused by AD and normal aging [4].

The progression of AD can be staged in three categories. Each stage is characterized by a unique set of symptoms that varies in severity. The early stage of the disease, also called pre-clinical stage, can last for more than a decade even before the manifestation of symptoms in the subjects. In this stage, there is no visible memory loss or behavioral changes. However, formation of abnormal proteins such as Amyloid plaques and neurofibrillary tangles takes place in certain sub-anatomic regions of the brain [5].

The second stage, referred to as Mild Cognitive Impairment (MCI), also known as the prodromal stage AD, is a transition stage between normal aging and AD, which is characterized by mild cognitive decline. The third phase is fully developed AD wherein the subjects suffer from severe loss of memory and challenges in executing daily routine works [6].

Neuroimaging is a promising way of research for diagnosing AD. The neuroimaging methods are widely used to study the manifestation of dementia. It is also being explored as an indicator of disease progression and as a surrogate marker to study the effectiveness of new therapies. Alterations occurring in the brain due to AD can be detected and quantified by Magnetic Resonance Imaging (MRI). The T1-weighted MRI differentiates the contrast between soft tissues of the brain and the skull. It also aids in the discrimination of white and gray matter structures and captures the information required for structural analysis of brain regions [7].

The ventricles are cavities situated in the center of the brain and are filled with Cerebrospinal Fluid (CSF). CSF provides a cushion for the brain, protecting it from damages caused internally or externally. The brain ventricles are surrounded by white and gray matter structures which are referred to as periventricular structures. Ventricular shape changes are considered as the most significant imaging biomarker for AD diagnosis compared to the morphometric changes in the whole brain or hippocampal region [8].

Corpus Callosum (CC) is located adjacent and superior to lateral ventricles. It is the largest fiber bundle connecting the two cerebral hemispheres. The passive enlargement of the lateral ventricle in AD directly results in the callosal arching and thinning resulting in callosal dysmorphology [9]. Thus, ventricular dilation might lead to deformations in CC that reflects the overall brain atrophic process.

Shape analysis contributes significant information on the description of brain regions, which is only grossly characterized by its volume. The shape of an object can complement volume and thickness measurements, while the shape features provide morphometric details of the structures [10]. The detection of the localized shape changes in CC could provide new insights about the structure-function relationships and assist in discovery of the underlying biological processes related to AD. The

quantitative analysis of these shape changes using appropriate descriptors could potentially lead to more accurate diagnosis of AD [11].

Recently, shape-based image descriptors using Laplace-Beltrami (LB) operators are employed as spectral signatures in the computational shape analysis. It captures information related to the intrinsic geometry of the objects [12]. The LB spectrum is represented as a set of squared frequencies that are associated to the eigen modes of a global oscillating membrane described on the manifold [13]. The LB eigenvalue shape features provide straightforward geometric interpretations of the objects or structures. Also, it contains valuable measures about the overall geometry of the objects [14].

In this work, the lateral ventricles and CC from normal, MCI, and Alzheimer subjects are extracted using reaction diffusion-based level set method (RDLSM). Further, LB eigenvalues are obtained from the segmented binary images to analyze the shape changes due to disease condition.

II. Methodology

In this work, T1-weighted MR images (Normal=92, MCI=63 and AD=29) are obtained from the public domain Open Access Series of Imaging Studies (OASIS) database. The images considered for this study are of resolution 1.0 x 1.0 x 1.25 mm^3 [15]. In this study, the mid-axial and midsagittal slices are considered as they provide the optimal view of the lateral ventricles and CC respectively.

The segmentation of the ventricle and CC in the T1-weighted MR images is attempted using RDLSM. Level sets are active contour models that have the capability of tracking complex deformations in the brain structures. In this method, a closed contour has been formulated as a zero-level set of a high dimensional function which undergoes motion dynamically to extract objects in the images. The mathematical description of RDLSM can be found here [16].

LB eigenvalue features are obtained from segmented ventricles and CC to quantify the structural variations due to AD. The inherent geometry of segmented (binary) brain sub-anatomic structures is associated with the spectrum of Laplace operators to illustrate the shape changes. The segmented images can be considered as a closed bounded domain $\Omega \subset R^d$ with piecewise smooth boundaries. For a binary image with foreground Ω, its equivalent Laplace operator is given by

$$\Delta_\Omega f \triangleq \sum_{i=1}^{d} \frac{\partial^2 f}{\partial x_i^2}, \ \forall X \in \Omega \quad (1)$$

where $X=[x_1,...,x_d]$ represent spatial coordinates. The eigenvalues and the eigenfunctions of Laplace operators are specified by the solutions of the Helmholtz equation with Dirichlet type boundary conditions. It is given by

$$\Delta f + \lambda f = 0, \ \forall X \in \Omega, f(X) = 0, \forall X \in \Omega, \quad (2)$$

where $\partial\Omega$ denotes boundary of the segmented sub-anatomic structure and $\lambda \in R$ is a scalar [17]. Mathematically there are an unlimited number of eigenvalues and functions that satisfy Eq. 2. The well-ordered collection of a positive eigenvalue series is given by

$$0 \leq \lambda_1 \leq \lambda_2 \leq \cdots \uparrow \infty. \quad (3)$$

The above series represents the continuum of binary images Δ_Ω. This set of eigenvalues comprise aspects of inherent geometry of segmented (binary) brain sub-anatomic structures [18]. The shape variations of the lateral ventricle and CC are extracted and correlated using this LB eigenvalue spectrum. Further, statistical analysis is carried out on the extracted LB eigenvalues to identify significant features that could distinguish MCI and Alzheimer subjects from normal aging.

III. Results and Discussion

Figure 1 represents typical transaxial view T1-weighted MR images for (a) normal, (b) MCI and (C) AD images. It is noted that in MR images the brain ventricles are situated in the center of the brain as one connected region with four horns and are enveloped by gray matter and white matter regions. They appear to be concave and dissimilar in shape from subject to subject causing difficulties in the segmentation. RDLSM has been used to segment ventricles in all the images. The details of the LSM parameter values in the initial contour evolution has been reported elsewhere [18]. Figure 1(d-f) shows the representative set of segmented ventricle images of normal, MCI and AD images respectively. As observed, the ventricle horns are found to be enlarged in the MCI and AD compared to the normal subjects. The size of the ventricle is evidently enlarged in AD subjects compared to MCI and normal. This might be due to the increment of CSF volume and in turn increased pressure on the ventricle surface.

Figure 2 shows the T1-weighted sagittal MR images of (a) normal, (b) MCI and (D) AD images. It is observed that CC lies as a roof on the ventricle with variations in shape and size throughout the structure. It is also observed that the thickness of CC varies among different subjects. For example, there is an apparent loss of neurons in the AD subject leading to colossal arching and thinning as shown in Figure 2(c). This may perhaps be due to Wallerian disintegration of commissural nerve fibers. The atrophy of CC results in functional debility of subjects due to decreased interhemispheric integration. The thickness of CC slightly changes with a rise in the disease progression. Figure 2(d-f) shows the representative set of segmented CC images of normal,

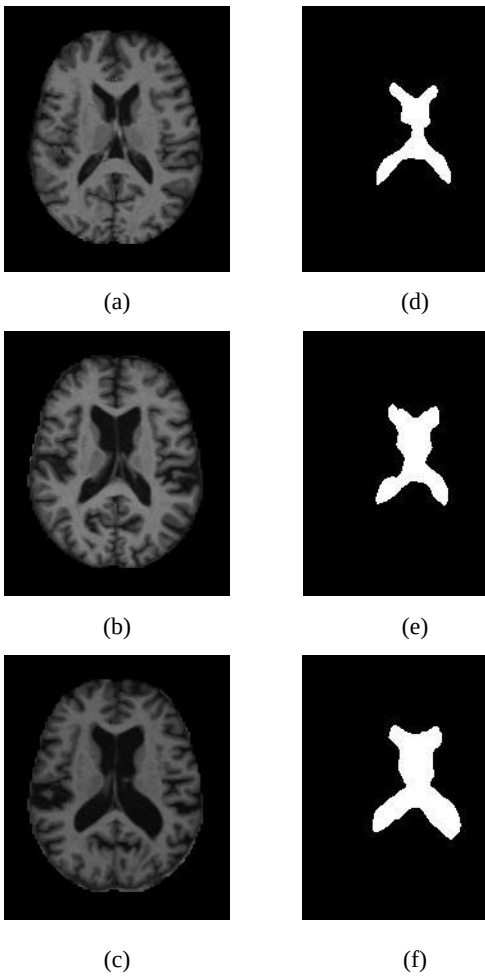

Figure 1. Representative set of (a) normal, (b) MCI, and (c) AD T1-weighted MR images and (d-f) their corresponding segmented ventricles.

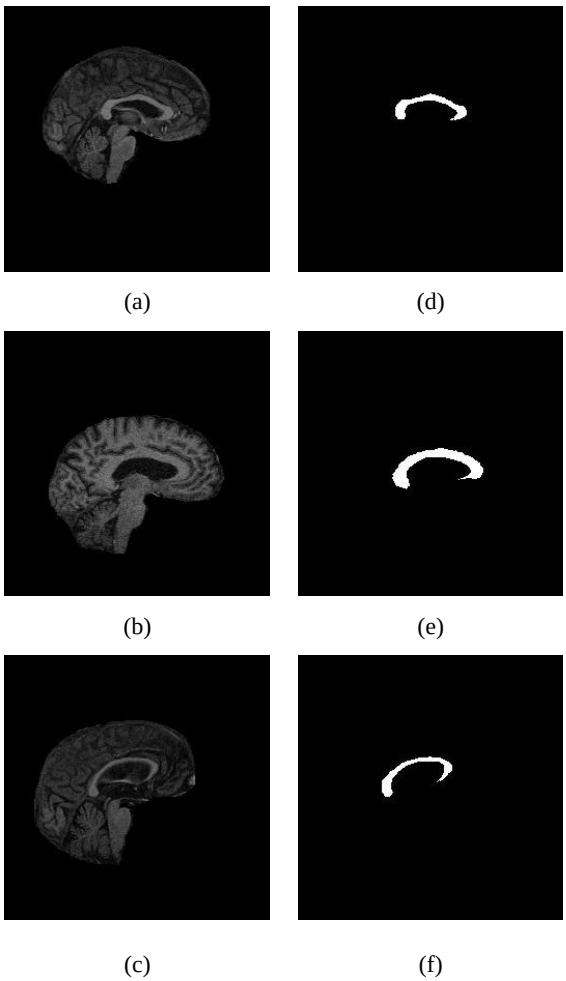

Figure 2. Representative set of (a) normal, (b) MCI, and (c) AD T1-weighted MR images and (e-f) their corresponding segmented CC.

MCI and AD images respectively. It is observed that segmented CC of AD subjects has greater atrophy compared to normal and MCI subjects. This could be due to Wallerian degeneration of axons in the white matter structures or direct myelin collapse of callosal fibers.

The frontal and occipital horns of the ventricle undergo size and as well as shape changes. This would cause atrophy in the CC. Although the degeneration takes place in CC, the variations are subtle and difficult to quantify. Therefore, LB eigenvalue signatures are used on segmented (binary) ventricle and CC images of normal, MCI and AD to quantify the shape changes.

Ten eigenvalues are obtained and normalized. The eigenvalues are presented in Table 1 and Table 2 for ventricle and CC respectively. The normalized LB eigenvalues are subjected to one-way analysis of variance (ANOVA) to analyze the statistical significance of features.

Table 1 shows that the LB eigenvalues λ_1 to λ_5 are statistically highly significant. In comparison it is observed that the LB eigenvalue λ_1 has a high significant value of $p < 8.11204E\text{-}10$. Consequently, the enlargement of ventricles in the MCI and Alzheimer subjects are distinctly reflected in the magnitude of mean values. It is also observed that, the mean eigenvalues are high for AD compared to normal and MCI subjects. A similar trend is observed between normal and MCI subjects. This might be due to the ability of LB eigenvalues in illustrating the enlargement of ventricles and particularly the dilation of frontal and occipital horns of ventricles.

Table 2 shows the statistical analysis of the LB eigenvalues for normal, MCI and AD subjects extracted from segmented CC images. The normalized features are statistically analyzed using one-way ANOVA. Among these, λ_2 and λ_3 are found to be statistically highly

Table 1. Statistical analysis of LB eigenvalues extracted from the segmented ventricle images

LB eigenvalues	Mean ± Standard deviation		
	Normal	MCI	AD
λ_1*	**0.36 ±0.12**	**0.40 ± 0.12**	**0.56 ± 0.50**
λ_2*	**0.36 ± 0.14**	**0.47 ± 0.15**	**0.59 ± 0.18**
λ_3*	**0.45 ± 0.16**	**0.53 ± 0.16**	**0.62 ± 0.13**
λ_4*	**0.39 ± 0.13**	**0.48 ± 0.17**	**0.52 ± 0.12**
λ_5*	**0.41 ± 0.15**	**0.50 ± 0.17**	**0.62 ± 0.12**
λ_6	0.46 ± 0.17	0.55 ± 0.18	0.64 ± 0.14
λ_7	0.45 ± 0.16	0.52 ± 0.17	0.63 ± 0.14
λ_8	0.43 ± 0.15	0 .51 ± 16	0.60 ± 0.12
λ_9	0.41 ± 0.13	0.51 ± 0.16	0.64 ± 0.13
λ_{10}	0.44 ± 0.16	0.54 ± 0.17	0.66 ± 0.13
* p<0.0001 (Statistically highly significant)			

Table 2. Statistical analysis of LB eigenvalues extracted from the segmented CC images

LB eigenvalues	Mean ± Standard deviation		
	Normal	MCI	AD
λ_1	0.63 ± 0.15	0.63 ± 0.12	0.62 ± 0.14
λ_2*	**0.67 ± 0.13**	**0.65 ± 0.15**	**0.63 ± 0.14**
λ_3*	**0.67 ± 0.15**	**0.66 ± 0.14**	**0.64 ± 0.16**
λ_4	0.65 ± 0.12	0.64 ± 0.12	0.63 ± 0.12
λ_5	0.68 ± 0.14	0.67 ± 0.12	0.67 ± 0.16
λ_6	0.65 ± 0.15	0.65 ± 0.12	0.63 ± 0.17
λ_7	0.61 ± 0.17	0.60 ± 0.11	0.59 ± 0.11
λ_8	0.64 ± 0.13	0.62 ± 0.10	0.62 ± 0.17
λ_9	0.66 ± 0.12	0.66 ± 0.10	0.64 ± 0.17
λ_{10}	0.65 ± 0.13	0.65 ± 0.12	0.64 ± 0.11
* p<0.0001 (Statistically highly significant)			

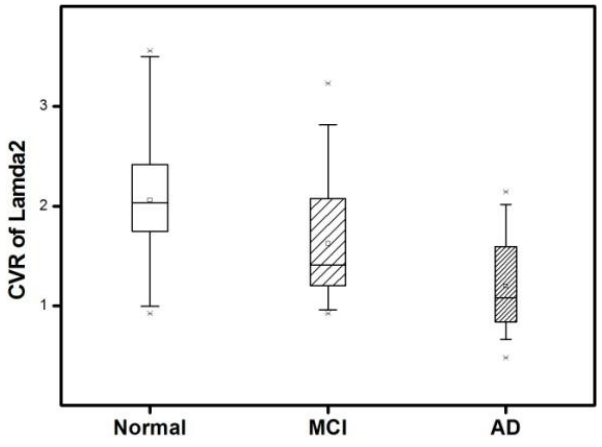

(a)

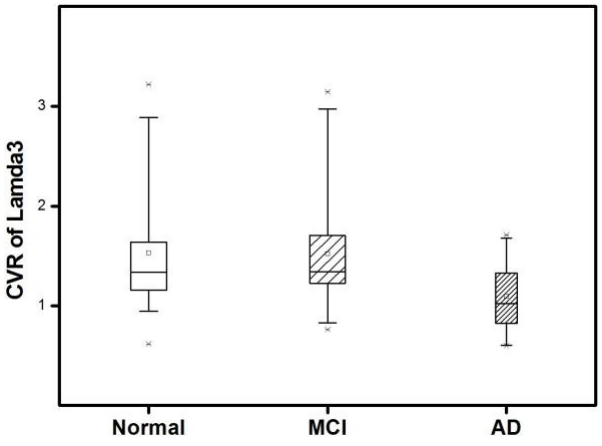

(b)

Figure 3. Comparison of CC to ventricle ratio for normal, MCI and AD subjects using (a) λ_2 and (b) λ_3

significant. It is observed that the mean eigenvalues of normal subjects are high in magnitude compared to MCI and AD subjects. This might be due to the capacity of the eigenvalues in signifying the callosal alterations that are caused due to the micro-structural neuronal degeneration. These micro-structural variations are better reflected by λ_2 than λ_3.

The enlargement of the ventricle has caused atrophy in CC thereby leading to Wallerian degeneration of nerve fibers and death of axons. Therefore, it is possible to quantify the structural changes of ventricles and CC in a metric. CC to Ventricle Ratio (CVR) has been formulated using statistically significant LB eigenvalues to describe the intrinsic geometric changes of brain regions. The CVR values for the eigenvalues λ_2 and λ_3 are shown in Figures 3 (a-b).

It is observed that the CVR of λ_2 shows high demarcation of MCI from the normal and AD patients. The obtained CVR illustrates the phenomenal atrophy of CC caused due to the ventricle enlargement. This ratio also shows the relationship and dependency of ventricle enlargement in the CC atrophy and describes the shape changes. This is an important ratio in the disease diagnosis as it considers both CC and ventricle in the shape analysis.

IV. Conclusions

In this work, the shape changes of ventricle and CC in Alzheimer's MR brain images are analyzed using LB eigenvalues. The eigenvalues λ_1 to λ_5 extracted from the segmented ventricles are found to reflect the ventricular enlargement in AD. Similarly, λ_2 and λ_3 are found to capture the deformations in CC of MCI and AD subjects. This demonstrates the ability of LB spectrum in elucidating the shape changes of dilated ventricles and callosal atrophy in MCI and Alzheimer subjects. Similarly, the formulated CVR values of λ_2 can statistically differentiate the normal from MCI and

Alzheimer subjects. This ratio also attempts to explain the phenomenon of atrophy of CC caused by the enlargement of ventricles in the normal, MCI and Alzheimer subjects.

REFERENCES

[1] X. Sheng, H. Chen, P. Shao, R. Qin, H. Zhao, Y. Xu, and F. Bai, "Brain structural Network compensation is associated with cognitive impairment and Alzheimer's disease pathology," *Frontiers in Neuroscience*, vol. 15, 2021.

[2] J. E. Galvin, P. Aisen, J. B. Langbaum, E. Rodriguez, M. Sabbagh, R. Stefanacci, R. A. Stern, E. A. Vassey, A. de Wilde, N. West, and I. Rubino, "Early stages of alzheimer's disease: Evolving the care team for optimal patient management," *Frontiers in Neurology*, vol. 11, 2021.

[3] P. Vannini, B. J. Hanseeuw, J. R. Gatchel, S. A. Sikkes, D. Alzate, Y. Zuluaga, S. Moreno, L. Mendez, A. Baena, P. Ospina-Lopera, V. Tirado, E. Henao, N. Acosta-Baena, M. Giraldo, F. Lopera, and Y. T. Quiroz, "Trajectory of unawareness of memory decline in individuals with autosomal dominant alzheimer disease," *JAMA Network Open*, vol. 3, no. 12, 2020.

[4] D. A. McGrowder, F. Miller, K. Vaz, C. Nwokocha, C. Wilson-Clarke, M. Anderson-Cross, J. Brown, L. Anderson-Jackson, L. Williams, L. Latore, R. Thompson, and R. Alexander-Lindo, "Cerebrospinal fluid biomarkers of Alzheimer's Disease: Current evidence and future perspectives," *Brain Sciences*, vol. 11, no. 2, p. 215, 2021.

[5] R. N. Martins, V. Villemagne, H. R. Sohrabi et al., "Alzheimer's disease: A journey from Amyloid peptides and oxidative stress, to Biomarker technologies and disease Prevention Strategies—Gains from AIBL and DIAN cohort studies," *Journal of Alzheimer's Disease*, vol. 62, no. 3, pp. 965–992, 2018.

[6] X. Wang, W. Huang, L. Su, Y. Xing, F. Jessen, Y. Sun, N. Shu, and Y. Han, "Neuroimaging advances regarding subjective cognitive decline in preclinical alzheimer's disease," *Molecular Neurodegeneration*, vol. 15, no. 1, 2020.

[7] R. Mohanty, G. Mårtensson, K. Poulakis, J.-S. Muehlboeck, E. Rodriguez-Vieitez, K. Chiotis, M. J. Grothe, A. Nordberg, D. Ferreira, and E. Westman, "Comparison of subtyping methods for neuroimaging studies in alzheimer's disease: A call for harmonization," *Brain Communications*, 2020. vol. 2,2 fcaa192.

[8] W. M. van Oostveen and E. C. de Lange, "Imaging techniques in Alzheimer's disease: A review of applications in early diagnosis and longitudinal monitoring," *International Journal of Molecular Sciences*, vol. 22, no. 4, p. 2110, 2021.

[9] S. Mangalore, S. S. Mukku, S. Vankayalapati, P. T. Sivakumar, and M. Varghese, "Shape profile of corpus Callosum as a signature to Phenotype Different Dementia," *Journal of Neurosciences in Rural Practice*, vol. 12, no. 01, pp. 185–192, 2020.

[10] C. Wachinger, et al. "BrainPrint: A discriminative characterization of brain morphology." *NeuroImage*, vol. 109, pp. 232-248, 2015.

[11] A. Rao, P. Aljabar, and D. Rueckert, "Hierarchical statistical shape analysis and prediction of sub-cortical brain structures," *Medical Image Analysis*, vol. 12, no. 1, pp. 55–68, 2008.

[12] M. Reuter, S. Biasotti, D. Giorgi, G. Patanè, and M. Spagnuolo, "Discrete Laplace–Beltrami operators for shape analysis and segmentation," *Computers & Graphics*, vol. 33, no. 3, pp. 381–390, 2009.

[13] M. Reuter, F.-E. Wolter, and N. Peinecke, "Laplace–beltrami spectra as 'shape-dna' of surfaces and solids," *Computer-Aided Design*, vol. 38, no. 4, pp. 342–366, 2006.

[14] M. Niethammer, M. Reuter, F.-E. Wolter, S. Bouix, N. Peinecke, M.-S. Koo, and M. E. Shenton, "Global medical shape analysis using the Laplace-Beltrami Spectrum," *Medical Image Computing and Computer-Assisted Intervention – MICCAI*, pp. 850–85, 2007.

[15] D. S. Marcus, T. H. Wang, J. Parker, J. G. Csernansky, J. C. Morris, and R. L. Buckner, "Open access series of imaging Studies (OASIS): Cross-sectional MRI data in young, middle aged, nondemented, and demented older adults," *Journal of Cognitive Neuroscience*, vol. 19, no. 9, pp. 1498–1507, 2007.

[16] K. Zhang, L. Zhang, H. Song, and D. Zhang, "Reinitialization-free level set evolution via reaction diffusion," *IEEE Transactions on Image Processing*, vol. 22, no. 1, pp. 258–271, 2013.

[17] K. R. Anandh, C. M. Sujatha, and S. Ramakrishnan. "Laplace Beltrami eigen value based classification of normal and Alzheimer MR images using parametric and non-parametric classifiers." *Expert Systems with Applications*, vol. 59, pp. 208-216, 2016.

[18] K. R Anandh, C. M. Sujatha, and S. Ramakrishnan. "A method to differentiate mild cognitive impairment and Alzheimer in MR images using Eigenvalue descriptors." *Journal of Medical Systems*, vol. 40, pp. 1-8, 2016.